World Academy of Science, Engineering and Technology
International Journal of Industrial and Manufacturing Engineering
Vol:9, No:1, 2015

Flow Behavior and Performances of Centrifugal Compressor Stage Vaneless Diffusers

Y. Galerkin, O. Solovieva

Abstract**—**Parameters of flow are calculated in vaneless diffusers with relative width 0,014–0,10. Inlet angles of flow and similarity criteria were varied. There is information on flow separation, boundary layer development, configuration of streamlines. Polytrophic efficiency, loss coefficient and recovery coefficient are used to compare effectiveness of diffusers. The sample of optimization of narrow diffuser with conical walls is presented. Three wide diffusers with narrowing walls are compared. The work is made in the R&D laboratory "Gas dynamics of turbo machines" of the TU SPb.

Keywords**—**Vaneless diffuser, relative width, flow angle, flow separation, loss coefficient, similarity criteria.

NOMENCLATURE

b - width of channel
c - velocity
c_r - radial velocity
c_u - tangential velocity
D - diameter
h_T - head
k - isentropic coefficient
K_n - specific speed
l - length
$\overline{m}$ - mass flow
M_c - Mach number
n - rotor rotation per second
p - pressure
r - radius
Re_{D2} - Reynolds number
T - temperature
u - circumferential velocity
α - flow angle
Φ - flow rate coefficient -
η - efficiency
λ_c - velocity coefficient
ν - kinetic viscosity
ϑ - divergence angle
ρ - density
ξ - recovery coefficient
ψ_T - work coefficient
ζ - loss coefficient

Abbreviations, Subscripts and Superscripts:

2 - impeller outlet section, vaneless diffuser inlet section
3 - vaneless diffuser discharge section
calc - calculated
des - design
imp - impeller
sep - separation
VLD - vaneless diffuser
$\overline{\ }$ - linear size, referred to D_2
* - total temperature, total pressure

I. OBJECTS OF THE WORK

Industrial centrifugal compressors are widely applied in all basic industries. Their summarily installed power is measured by dozens of millions KWt in industrial countries. Effective gas dynamic design methods are important to economy of energy. Vaneless diffusers are important part of a stage flow path. Fig. 1 shows its disposition in a typical industrial compressor stage.

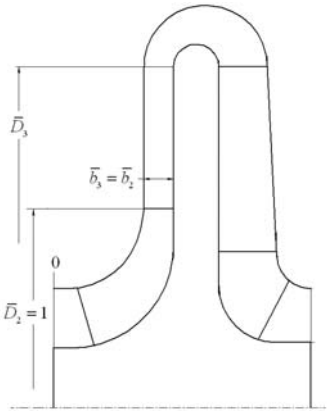

Fig. 1 Vaneless diffuser disposition in a centrifugal compressor stage and its dimensions

The diffuser starts at the diameter of the impeller exit $\overline{D}_2 = 1,0$ and continues to the diameter $\overline{D}_3$ where a return channel starts. Its width $\overline{b}_3 = \overline{b}_2$ is constant along radius that is not an optimal solution in many cases.

A diffuser transforms to pressure excessive kinetic energy produced by an impeller. Its role in effective compressor operation is sufficient. Correct flow parameter calculation in a vaneless diffuser is a part of the problem. The general information on VLD principles of operation and design is

Yuri Borisovich Galerkin is with S.-Peterbugd Poltechnical Yniversity, Russian Federaton (phone: +7-921-942-73-40; fax: 8-812-552-86-43; e-mail: yuiri_galerkin@ mal.ru).

Olga Anatolievna Solovieva is with S.-Peterbugd Poltechnical Yniversity, Russian Federaton (phone: +7-812-552-86-43 fax: 8-812-552-86-43; e-mail: osochka-88@mail.ru).

presented in [1], [2]. Modeling experience is presented in [3]. The aim of this work is to collect more information about flow behavior and head losses. The information can be used for Math models in proper computer programs. The objects of numerical analysis were valeless diffusers with parallel walls mainly, i.e. diffusers with constant width along radius.

Flow in diffusers with relative width $\bar{b}_2$ = 0,014, 0,019, 0,025, 0,029, 0,033, 0,043, 0,057, 0,074, 0,10 and relative length $\bar{D}_3$ = 1,6 was calculated with inlet flow angles α_2 =10 – 45^0.

Similarity criteria were varied in range $\lambda_{c2} = \frac{c_2}{\sqrt{\frac{2k}{k+1} RT_2^*}} =$ 0,23 – 0,82, $\mathrm{Re}_{D2} = \frac{c_2 D_2}{\nu_2}$ =3,8E6 – 10,3E6 with constant k = 1,4. Surfaces were hydraulically smooth.

H-type structured nets with 225216 elements were created with the program ANSYS CFX 14,0 and the net generator ICEM. Turbulence model $k-\varepsilon$ was applied to calculations.

II. Efficiency Parameters

In [4] loss coefficient was calculated using an approximate formula:

$$\varsigma_{app} = \frac{p_1^* - p_2^*}{0{,}25(\rho_1 + \rho_2)c_1^2}, \quad (1)$$

The reasons for the adoption of simplified relationship was the consideration that at low Mach numbers loss calculation with the definition of the polytrophic exponent may be incorrect due to inaccuracy of temperatures and pressures in the iterative calculation process.

In the absence of heat exchange a ratio to calculate the polytrophic efficiency of the diffuser operating with compressible flow is:

$$\eta = \frac{\ln(p_3/p_2)}{\frac{\kappa}{\kappa-1}\ln(T_3/T_2)}, \quad (2)$$

Loss coefficient and efficiency are connected by:

$$\eta = 1 - \frac{\varsigma}{1-\left(\frac{c_3}{c_2}\right)^2}, \quad (3)$$

or

$$\zeta = 1 - \frac{\eta}{1 - 0{,}5\left(c_3^2/c_2^2\right)}. \quad (4)$$

Performance curves calculated by (1)-(4) are presented at Fig. 2.

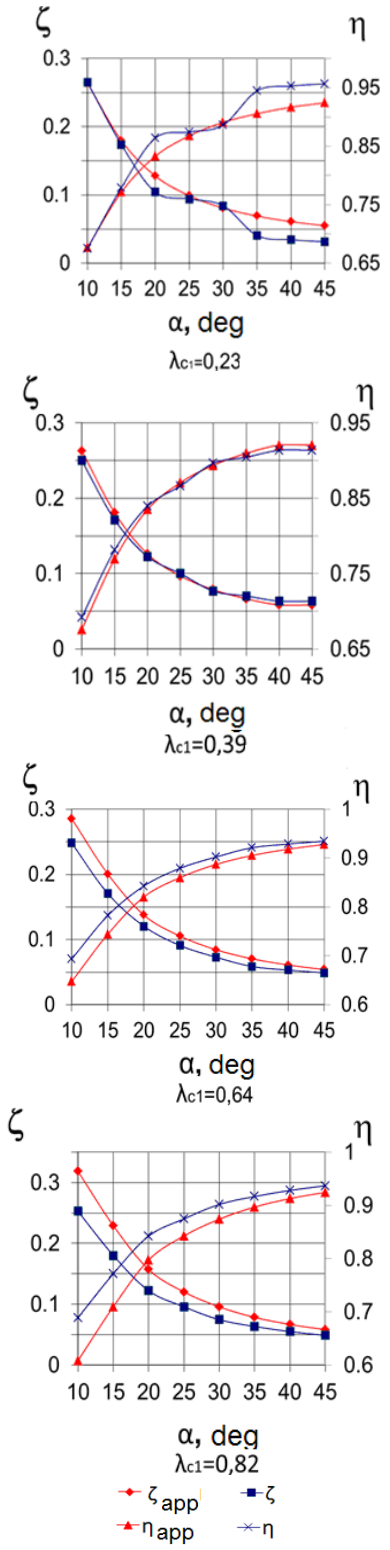

Fig. 2 Diffuser performance curves computed with precise and approximate formulae $\bar{b}_2$ = 0,057

Calculations confirmed the ineffectiveness of compressible flow formulae for λ_{c2} = 0.23. For λ_{c2} = 0.39 both calculations

give almost the same result. So, we can assume that approximate formula (1) should be used for $\lambda_{c2} \le 0.40$.

The recovery coefficient shows what part of a kinetic energy of flow is transformed to the polytrophic head:

$$\xi = 1 - \frac{\eta}{1 - 0{,}5\left(c_3^2 / c_2^2\right)}. \quad (5)$$

III. Flow Structure

Fig. 3 presents meridian streamlines in diffusers with different width at different inlet angles.

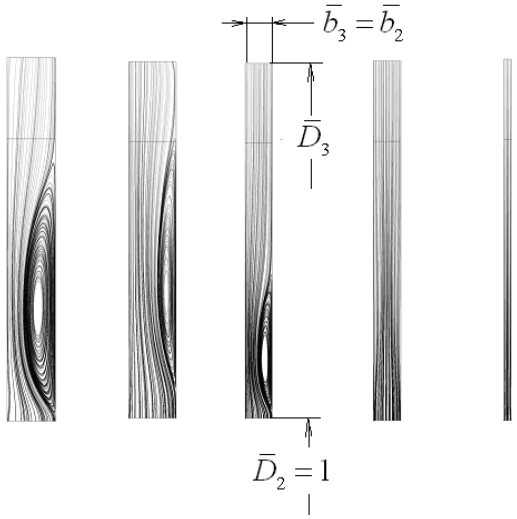

Fig. 3 Meridian streamlines in diffusers with different width at different inlet angles. From left to right: $\bar{b}_2 = 0{,}10$, $\alpha_2 = 10$ and 20^0, $\bar{b}_2 = 0{,}057$, $\alpha_2 = 10^0$, $\bar{b}_2 = 0{,}014$, $\alpha_2 = 10^0$, $\lambda_{c2} = 0{,}64$, $\mathrm{Re}_{D2} =$ 9,1E+6

Flow separation occurs in wide diffusers when flow angles are low. Separation does not occur at any conditions in diffusers with $\bar{b}_2 \le 0{,}022$. High level of shear stresses due to closeness of walls prevents separation but leads to lower efficiency. Separation occurs at points where shear stress is equal to zero. It happens in wider diffusers at lower flow angles. Pressure gradient is directed along a radius because both velocity components are creating pressure gradient in this direction [1]:

$$\frac{1}{\rho}\frac{dp}{dr} = -c_r \frac{dc_r}{dr} + \frac{c_u^2}{r} \approx \frac{c^2}{r}. \quad (6)$$

A velocity radial component changes its direction to the opposite one in a separation zone. A tangential component magnitude and direction is the same in a core flow and in a separation zone.

The lower is an inlet angle – the lower is a radial velocity and its shear stress that resists to separation. The sample of shear stresses when separation takes place is shown at Fig. 4.

Shear stresses are negative in a separation zone as the velocity tangential component is negative there.

The wider is a diffuser the bigger is an angle that corresponds to flow separation start – Fig. 4. Fig. 4 shows that this angle is 10^0 and 15^0 for $\bar{b}_2 =$ 0,029 and 0,057 and is independent of the velocity coefficient. For the diffuser with $\bar{b}_2 =$ 0,10 the separation angle is bigger for bigger velocity coefficient. It is equal to 25^0 at $\lambda_{c2} =$ 0,82. In wide diffusers and at high velocity coefficients separation starts at bigger flow rate as a flow rate is proportional to value of $\sin\alpha_2$: $\bar{m} = \rho_2 \pi D_2 b_2 c_2 \sin\alpha_2$.

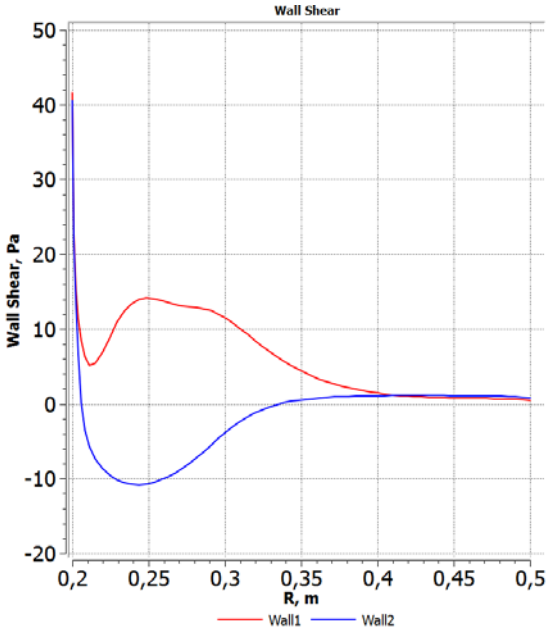

Fig. 4 Shear stress radial component at walls of the diffuser: $\bar{b}_2 =$ 0,057, $\alpha_2 = 10^0$, $\lambda_{c2} =$0.64, $\mathrm{Re}_{D2} =$ 9,1E6

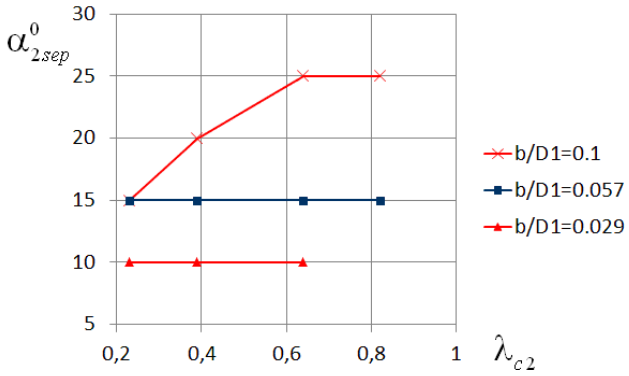

Fig. 5 Inlet flow angle α_{2sep} corresponding to separation start versus inlet velocity coefficient for diffusers with three relative widths

Flow separation leads to head losses. Just more dangerous are unsteady forces due to separation unsteady character. Flow separation in vaneless diffuser leads to surge of a stage usually that makes a compressor operation impossible. The known

way to avoid separation is to apply a diffuser with tampering walls: $b_3 < b_2$.

The popular opinion is that a flow consists of boundary layers and non viscid core in wide diffusers. The calculations demonstrate that the core disappears at some distance from an entrance in all diffusers – in wide diffusers too. An initial part of a diffuser where boundary layers still exist is shorter in narrow diffusers and at lower inlet angles – Figs. 5, 6.

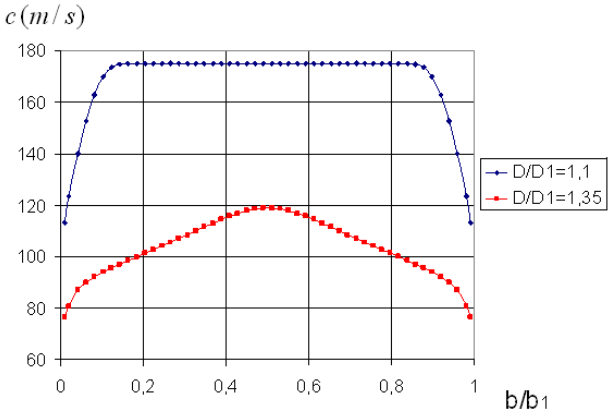

Fig. 6 Velocity profiles in the diffuser with $\bar{b}_2 = 0{,}057$ on two relative radiuses. $\alpha_2 = 20^0$, λ_{c2} =0.64, $\mathrm{Re}_{D2} = 9{,}1\mathrm{E}{+}6$

IV. Performance Curves Presentation

Diffusers with different relative width are intended for stages of proper specific speed. The specific speed coefficient is a function of mass flow rate, head and an impeller speed of rotation. The specific speed connects dimensional and non dimensional parameters of a stage [5]:

$$K_n = 2\sqrt{\pi}\frac{\left(\bar{m}/\rho_0^*\right)^{0,5}}{h_T^{0,75}} n\left(1/s\right) = \frac{\Phi^{0,5}}{\psi_T^{0,75}}. \qquad (6)$$

The flow rate coefficient is $\Phi = \dfrac{\bar{m}}{\rho_0^* \dfrac{\pi}{4} D_2^2 u_2}$, work coefficient is $\psi_T = \dfrac{c_{u2}}{u_2}$. Their values determine expected efficiency and shape of gas dynamic performance curves [1], [5]. Values of Φ_{des} and ψ_{Tdes} must be chosen at the start of design of an impeller. Flow parameters at an exit of an impeller are defined in a process of design.

Flow rate coefficient at an impeller exit is connected with a flow rate coefficient on its inlet:

$$\Phi_2 = \frac{\bar{V}_2 = \pi D_2 b_2 c_{r2}}{\dfrac{\pi}{4} D_2^2 u_2} = 4\pi \bar{b}_2 \varphi_2 = \Phi \frac{\rho_2}{\rho_0^*}. \qquad (7)$$

Coefficients Φ_2 and ψ_T are connected with parameters that define flow rate through a vaneless diffuser: $\Phi_2 = 4\pi \bar{b}_2 \varphi_2 = 4\pi \bar{b}_2 \psi_T tg\alpha_2$. Therefore the flow rate parameter for vaneless diffuser we present as:

$$\Phi_2 / \psi_T = 4 \cdot \bar{b}_2 \cdot tg\alpha_2. \qquad (8)$$

Performance curves and deceleration of flow in diffusers with $\bar{b}_2 = 0{,}014 - 0{,}10$ are presented at Figs. 7, 8 as functions of Φ_2 / ψ_T.

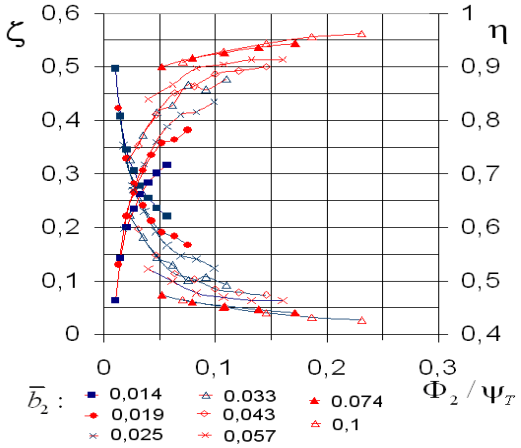

Fig. 7 Loss coefficient and coefficient of efficiency versus flow rate factor for diffusers with $\bar{b}_2$ =0,014…0,100, $\bar{D}_3 = 1{,}60$, λ_{c2} =0,39, Re_{D2}=6,2E6

Only the regimes without separation of flow are presented on the graphics. It is evident that wide diffusers with $\bar{b}_2 = 0{,}10$ and 0,074 are very effective in all zone of the flow rate parameter Φ_2 / ψ_T.

The narrower a diffuser is - the less is its effectiveness due to friction losses. Strong flow deceleration is not a positive factor in narrow diffusers. It is a result of a tangential component of velocity loss due to friction.

V. Meridian Shape Optimization

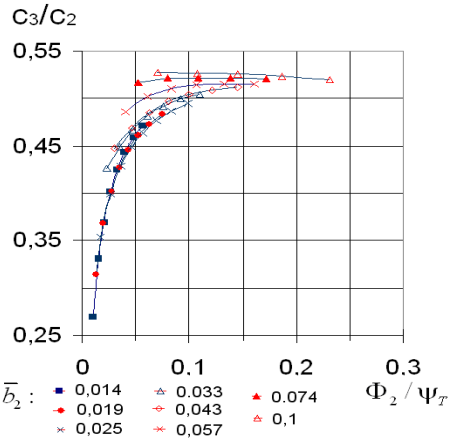

Fig. 8 Ratio c_3 / c_2 versus flow rate factor for diffusers with $\bar{b}_2$ = 0,014…0,100, $\bar{D}_3 = 1{,}60$, λ_{c2} =0,39, Re_{D2}=6,2E6

There is no separation of flow in narrow diffusers but friction losses are excessive. These losses are smaller in diffusers with increased width along radius. It is possible to widen a narrow diffuser to some level without separation of flow.

Four variants of the diffuser with $\bar{b}_2 = 0{,}014$ and $\bar{b}_3 > \bar{b}_2$ were analyzed. The diffusers have straight conical walls with the divergence angle $\vartheta = 0{,}46^0$, $2{,}0^0$, $4{,}0^0$, $6{,}0^0$. The configuration of a conical diffuser demonstrates Fig. 9.

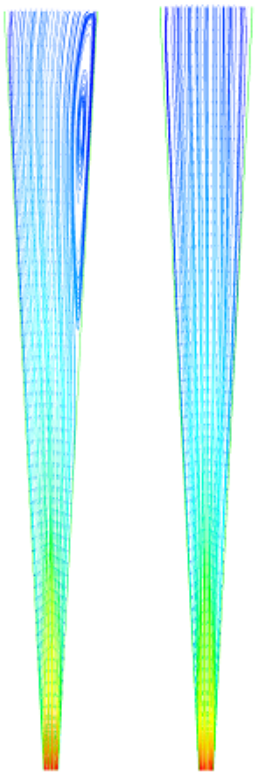

$\alpha_2 = 30^0$ $\alpha_2 = 45^0$

Fig. 9 Meridian configuration of the conical diffuser with $\bar{b}_2 = 0{,}014$ and $\vartheta = 6^0$. Meridian streamlines are presented at two inlet angles. $\overline{D_3} = 1{,}60$, $\lambda_{c2} = 0{,}64$, $\mathrm{Re}_{D2} = 9{,}1\mathrm{E}6$

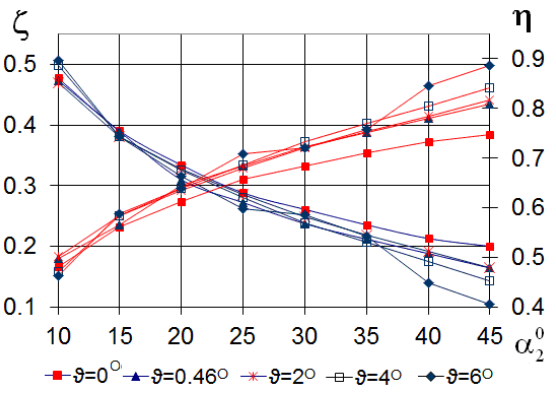

Fig. 10 Performance curves of diffusers with different divergence angles $\bar{b}_2 = 0{,}014$, $\overline{D_3} = 1{,}60$, $\lambda_{c2} = 0{,}64$, $\mathrm{Re}_{D2} = 9{,}1\mathrm{E}6$

The meridian streamlines demonstrates that flow separation occurs in the diffuser with wall divergence angle 6^0. It takes place at inlet angles $\alpha_2 \le 35^0$. The separation takes place in the diffuser with $\vartheta = 4^0$ also. There is no flow separation in the diffusers with $\vartheta = 0{,}46^0$ and $2{,}0^0$.

Fig. 10 presents efficiency and loss coefficient performance curves of four diffusers.

The diffusers with $\vartheta = 4{,}00$ and $6{,}00$ are most effective at flow inlet angles more that 20^0. But the flow separation takes place in them at flow inlet angles corresponding to practically important flow rates. Diffusers with flow separation cannot be recommended to practical application. .

Flow in the diffusers with $\vartheta = 0{,}46^0$ and $2{,}0^0$ is not separated at any angle of flow. They both are more effective that the diffuser with constant width at $\alpha_2 > 15^0$. The diffuser with $\vartheta = 2{,}0^0$ can be recommended for design practice as it has the same loss coefficient as the diffuser with $\vartheta = 0^0$ at $\alpha_2 < 15^0$. Its recovery coefficient is the same practically as of diffusers with $\vartheta = 4{,}0^0$ and $6{,}0^0$ – Fig. 11.

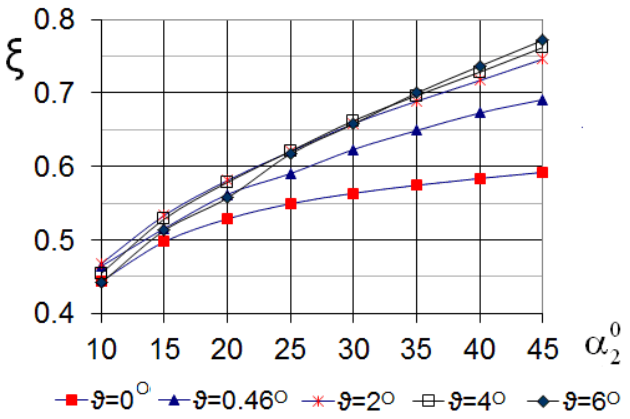

Fig. 11 Recovery coefficient of diffusers with different divergence angles $\bar{b}_2 = 0{,}014$, $\overline{D_3} = 1{,}60$, $\lambda_{c2} = 0{,}64$, $\mathrm{Re}_{D2} = 9{,}1\mathrm{E}6$

Calculations show that in diffusers with $\bar{b}_2$ less than 0.022, flow separation does not occur even when the flow angle is 10^0. In wide diffusers radial component of the velocity gets the opposite direction when flow angles are less than 20 - 25^0. These values correspond to design regime for many impellers. Diffusers with narrowed initial part are recommended to match impellers [4], [5]. The four VLD variants with the same relative width $b_3 / D_2 = 0.0743$ and the radial length $D_3 / D_2 = 1{,}71$ are compared – Fig. 12:

- variant 1 with $b_2 = b_3$;
- variant 2 with $b_3 = 0{,}073 b_2$, narrowing on distance $\bar{l} = 0{,}081$ from one side;
- variant 3 with $b_3 = 0{,}073 b_2$, narrowing on distance $\bar{l} = 0{,}015$ from one side;
- variant 4 with $b_3 = 0{,}073 b_2$, narrowing on distance $\bar{l} = 0{,}015$ from both sides.

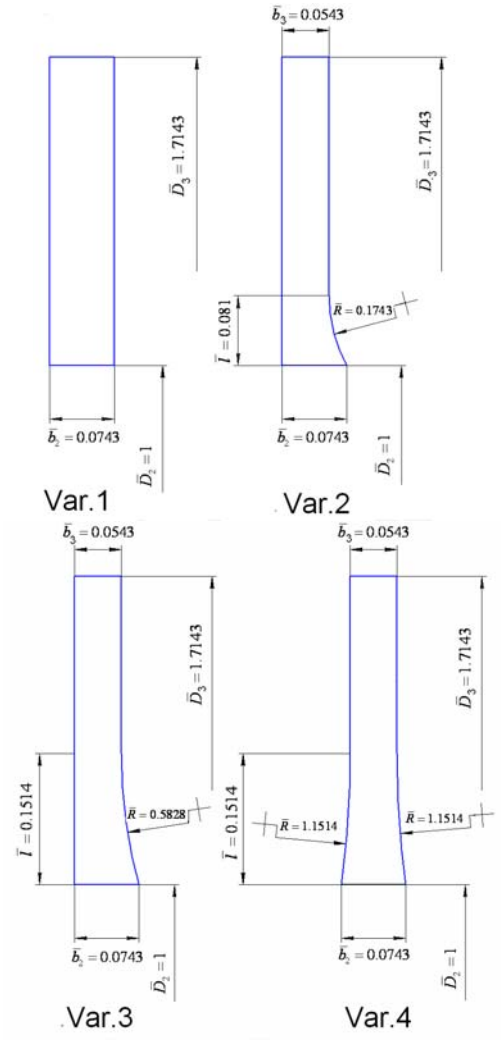

Fig. 12 Meridian shape of investigated VLD variants

Flow deceleration ratio is presented at Fig. 13. When the flow angle is 20^0 the flow deceleration in narrowed VLD is significantly less. When the flow angle is 45^0 the difference of deceleration ratios is drastic. The reason is that a radial component in the narrowed diffusers decreases too little.

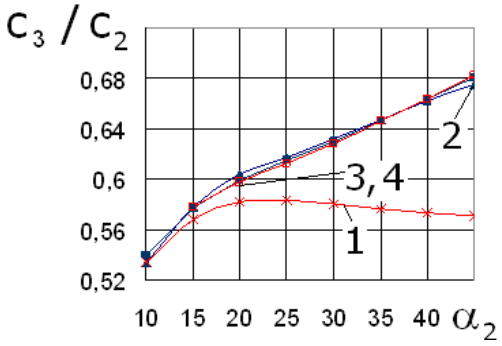

Fig. 13 Deceleration of the VLD flow depending on the flow inlet angle

Figs. 14, 15 present performance curves $\eta, \zeta = f(\alpha_2)$, $\xi = f(\alpha_2)$ of the four VLD variants.

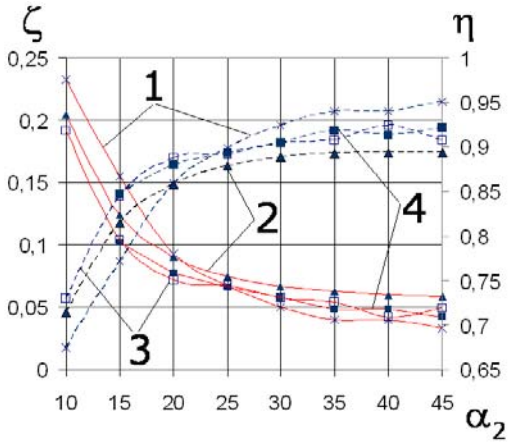

Fig. 14 Performances curves of four VLD variants

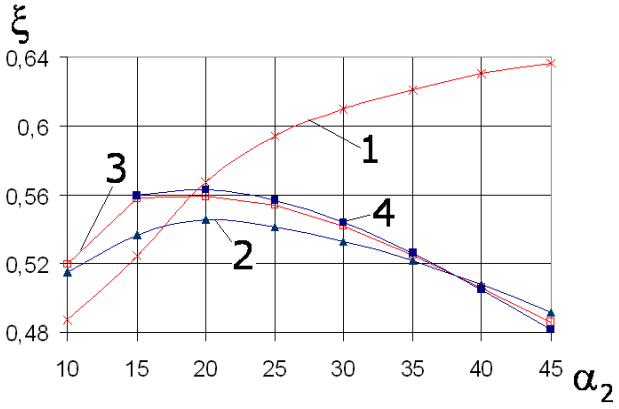

Fig. 15 Recovery coefficient depending on the inlet flow angle

Evidently when $\alpha_2 \geq 22^0$ VLD with constant width is more effective. Narrowed diffusers work better than a diffuser with constant width in its separation zone. Diffusers with the longer narrowing part (var. 3, 4) are better in all range of α_2 practically. Obviously the matching of a diffuser and an impeller can be achieved by proper choice of a diffuser width along radius.

REFERENCES

[1] Galerkin, Y.B. Tubrocompressors. (text) /Y.B.Galerkin// LTD information and publishing center. – Moscow. – KHT. -2010. – P. 596. (in Russian).
[2] Seleznev, K.P., Galerkin, Y.B. Centrifugal compressors. (text) /K.P. Seleznev, Y.B.Galerkin // Leningrad. – 1982. – P. 271. (in Russian).
[3] Y.B. Galerkin, K.V. Soldatova. Modeling of industrial compressor process of operation. Scientific background, stages of development, modern state. (text) /Y.B.Galerkin, K.V. Soldatova// STU. – SPb. - 2011. - P. 327.
[4] Y. Galerkin, O.A. Solovieva. Improvement of vaneless diffusers calculation based on CFD experiments. Part 1. // Compressors and pneumatics. 2014. – № 3. - |P. 35-41. (in Russian).
[5] Y.B. Galerkin, O.A. Solovieva. Improvement of vaneless diffusers calculation based on CFD experiments. Part 2. // Compressors and pneumatics, 2014. – № 4. – P. 15-21. (in Russian).